Journal of Applied Sciences

ISSN 1812-5654

science alert

ANSInet
an open access publisher
http://ansinet.com

Journal of Applied Sciences 6 (8): 1671-1678, 2006
ISSN 1812-5654
© 2006 Asian Network for Scientific Information

The Role of CeO_2 in the High Electric Field ZnO Varistors

[1]Ming Lei, [1]Shengtao Li, [1]Jianying Li and [2]Mohammad A. Alim
[1]State Key Laboratory of Electrical Insulation and Equipment,
Multi-disciplinary Materials Research Center,
Xi'an Jiaotong University, Xi'an 710049, People's Republic of China
[2]Department of Electrical Engineering, Alabama A and M University, P.O. Box 297,
Normal, Alabama 35762, USA

Abstract: The high electric field ZnO-Bi_2O_3 based varistor materials are developed using CeO_2 in the recipe. Achieving such varistors is commercially desired as the resulting device utilizes reduced volume of materials and thereby enhancing cost effectiveness. Although there may be a subtle role of the electrolytic nature of the CeO_2 in the form of ion transport within the secondary phases in the microstructures causing possible degradation, it is observed that the addition of CeO_2 plays a pivotal role for achieving high electric field varistors via reducing the average grain size to about 25%. The overall enhancement in the voltage gradient for such average grain size distribution exceeds 75%. The plausible role of the chemistry at the grain boundary interfaces for this observation is not ruled out beside the average grain size reduction. The voltage gradient is presumed to be the function of the grain size reduction and overall charge trapping at the grain boundary interfaces where the applied electric field is primarily experienced. The terminal capacitance-voltage (C-V) measurement as a function of applied frequency of the ac small-signal amplitude indicates strong influence of the trapping effect at the grain boundary interfaces assuming identical carrier density in the ZnO grains for each varistor material. The nonlinear coefficient obtained in the current-voltage (I-V) plot is not affected for the CeO_2 added varistors. The C-V data are confirming the presence of the back-to-back Schottky barrier as observed in the varistor samples without CeO_2.

Key words: ZnO varistors, electroceramics, ceria, high-field, microstructure

INTRODUCTION

Zinc oxide (ZnO) varistors with additives of Bi_2O_3, Sb_2O_3, Co_2O_3, MnO_2 and Cr_2O_3 are non-linear electroceramic components whose primary function is to sense and limit transient surges in a repeated manner (Matsuoka, 1971; Levinson and Philipp, 1986; Gupta, 1990). In general, a ZnO varistor arising from this type of base recipe has a breakdown electric field E_b ranging between 100 and 200 V mm^{-1} (Matsuoka, 1971; Eda, 1978). Usually the breakdown electric field is referred to the breakdown voltage gradient corresponding to 1 mA cm^{-2} (Alim *et al*., 1988a). High electric field (high-field or high voltage gradient) varistors have become technologically important because of their reduced volume and thus, use of low mass of materials and thereby enhancing cost effectiveness (Shichimiya *et al*., 1998). Ai *et al*. (1995) have reported high-field varistors of E_b ranging between 300 and 400 V mm^{-1} by modifying the proportion of the additives other than Bi_2O_3 in the base recipe. Several attempts have shown that varistors prepared with sub-micron (nano-size) ZnO particles and additive powders yield average grain size of about 2-3 μm and high voltage gradient 1000 V mm^{-1} (Viswanath *et al*., 1995; Ya *et al*., 1998). Recently, it has been reported that the incorporation of various Rare-earth Oxides (REO) such as Pr_6O_{11} or Y_2O_3 can significantly increase the breakdown field without debasing the performance of the varistors (McMillan *et al*., 1998; Bernik *et al*., 2001).

In this study electrical properties and microstructures of the high electric field CeO_2 added ZnO-Bi_2O_3 based varistors are reported. Also an attempt has been made to comprehend the role of the back-to-back grain boundary Schottky barriers in conjunction with the trapping response in the CeO_2 added ZnO varistors that caused high electric breakdown field. The novelty of this varistor recipe indicates a potential opportunity for making high electric field varistors possessing reduced volume for the same applications' rating.

MATERIALS AND METHODS

The base varistor samples comprising of 95.216 mole% ZnO, 0.5 mole% Bi_2O_3 and 4.284 mole% of Sb_2O_3,

Corresponding Author: Mohammad A. Alim, Department of Electrical Engineering, Alabama A and M University, P.O. Box 297, Normal, Alabama 35762, USA

Co_2O_3, MnO_2, Cr_2O_3, Ni_2O_3, SiO_2, B_2O_3 and Al_2O_3 are prepared. The modification of this recipe is made using x mole% of CeO_2 where x = 0.1, 0.3, 0.5 and 0.9 mole% to obtain varistor samples labeled as C1, C3, C5 and C9, respectively. The base varistor sample is designated as C0. Each recipe was used in making varistor samples using conventional electroceramic processing methods available in most published documents (Matsuoka, 1971; Levinson *et al.*, 1986; Gupta, 1990). The sintering operation was performed in normal ambient air for all the samples in the kiln using an average heating rate of 2°C min^{-1} up to 1175°C. After holding for 2 h at 1175°C the samples were cooled to 720°C using cooling rate of 1°C min^{-1} and then furnace cooled implying furnace shut off. The resulting varistor samples were ranging between 8.5 and 8.6 mm in diameter and 1.6 to 1.7 mm in thickness.

The additives are ball milled and brought to a uniform particle size distribution averaging about 1 micron for the additives and then dispersed with the ZnO powders having average particle size of about 1 μm. In general, average particle size affects the device's resulting functional capabilities via observed values in the pH of the slurry, heat development during dispersion of the additives with ZnO, period of dispersion, etc. Eventually, the spray dried powder is also influenced by the ultimate average particle size of the additives as well as ZnO. As such the resulting electrical property is influenced by these processing variables.

The loss of Bi_2O_3 in these devices during sintering is no different than the loss in the commercial setting as these varistor materials were prepared in such a condition. In fact, due to the loss in the sintering process Bi_2O_3 is added in such a way in the recipe that the net contribution to the microstructure remains intact and the resulting content remains desired in the device. Also, in order to protect the loss of Bi_2O_3 ceramic enclosed containers are used. Thus, the devices (varistor materials) used in this investigation are commercially processed in the manufacturing set up.

For the I-V measurement, both surfaces of the samples were coated with conductive Ag paste and annealed at 530°C for 20 min to obtain the ohmic contact. The nonlinear coefficient α is calculated using (Matsuoka, 1971):

$$\alpha = \frac{\log\left(I_2/I_1\right)}{\log\left(V_2/V_1\right)} = [\log (V_{1mA.cm}{}^{-2}/V_{0.1mA.cm}{}^{-2})]^{-1}, \quad (1)$$

where $V_{1mA.cm}{}^{-2}$ (= V_2) and $V_{0.1mA.cm}{}^{-2}$ (= V_1) are the voltages corresponding to the current density 1 $mA.cm^{-2}$ (= I_2) and 0.1 $mA.cm^{-2}$ (= I_1), respectively. The leakage current, I_L, is measured at V = 0.8 $V_{1mA.cm}{}^{-2}$ (80% $V_{1mA.cm}{}^{-2}$). The C-V measurement was conducted using an in-house built circuit that worked in a frequency range 100 Hz through 10 KHz at dc voltages up to 400 V. This is ac small-signal superimposed with applied dc voltage measurement and its frequency range was established on the basis of the time constant of the in-house built circuit similar to that used by Richmond (1980).

For the microstructure investigation using scanning electron microscope, the surface of the sintered bodies were first polished to mirror-like and then lightly etched with HCl solution at room temperature. These surfaces were then examined with a Scanning Electron Microscope (SEM: Philips XL-20, Netherlands) in the Backscattered Electron (BSE) mode. The average grain size D was determined by the Mendelson intercept (Mendelson, 1969) method. Later the crystalline phases were determined by the powder X-ray diffraction (XRD, Cu K_α radiation: Rigaku D/MAX-3C, Japan) analysis.

RESULTS AND DISCUSSION

Current-voltage (I-V) behavior: Figure 1 shows the I-V behaviors (in J-E denotation) of the C0, C1 and C9 samples. For each sample, the ohmic region is very prominent exhibiting very slow or low gradual increment of the nonlinear coefficient up to a certain electric field (such as about 300 V mm^{-1} for C1 sample) and then

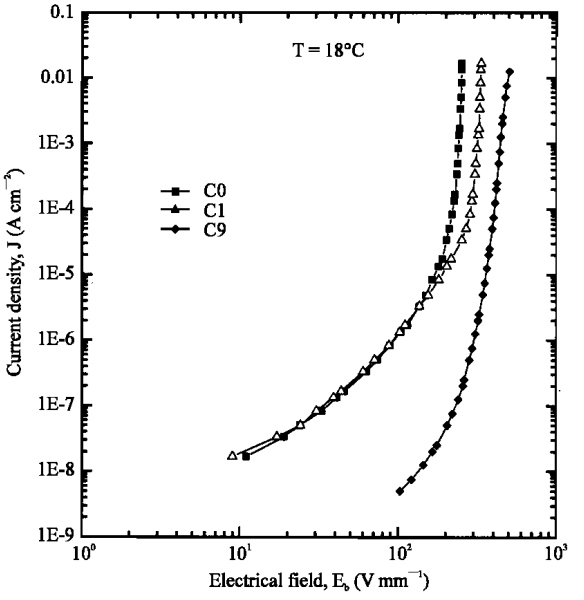

Fig. 1: Current-voltage response of the ZnO-Bi_2O_3 based varistors containing 0 mole% CeO_2 (C0: base varistor), 0.1 mole% CeO_2 (C1) and 0.9 mole% CeO_2 (C9)

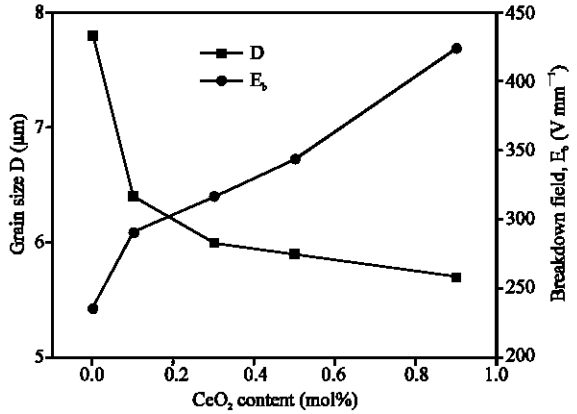

Fig. 2: Dependence of CeO_2 content on the ZnO grain size D and the breakdown field E_b

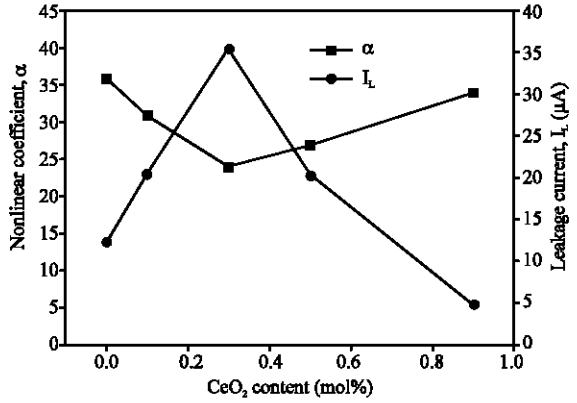

Fig. 3: Nonlinear coefficient α and leakage current I_L versus CeO_2 content

breakdown occurs in a narrow electric field range. This is favorable indication in terms of protective margin under transient over-voltage situation of the device. The calculated nonlinear coefficient and breakdown field of sample C0 are 37 and 236 V mm^{-1} whereas for C9 are 35 and 425 V mm^{-1}, respectively. This shows that the addition of CeO_2 with 0.9 mole% can significantly enhance the breakdown field of ZnO-Bi_2O_3 based varistors without greatly impairing their nonlinear characteristics.

The breakdown field E_b variations with the content of CeO_2 are shown in Fig. 2. The grain size variations are also plotted for comparison. It can be seen that the average ZnO grain size was decreased from 7.8 to 5.7 μm, while the breakdown field (E_b) increased substantially from about 235 to about 425 V mm^{-1}. Considering the high melting point of CeO_2 (about 2600°C), it is unlikely to have liquid phase as Bi_2O_3 does experience at these sintering temperatures. Actually the ratio of final density (ρ) and theoretical density (ρ_t) of the samples decreased monotonically from 96 to 95% (of the theoretical density, concrete values are not presented here) at these temperatures as CeO_2 content increased. These results when combined with the distribution of the CeO_2 phase have made one postulate that the newly introduced CeO_2 particles pinned at the grain boundaries during sintering and bounded the liquid-phase sintering behavior of Bi_2O_3. Thus, it hindered the mass transportation during the sintering cycle and restricted the grain growth substantially. The observed behavior of the grain growth inhibition incorporating CeO_2 in the recipe is separate behavior that was confirmed in the literature with the addition of Sb_2O_3.

In comparison to the drastic change in E_b, the nonlinear coefficient α did not change substantially and remained at 30±6. These parameters are displayed in Fig. 3 with increasing CeO_2 content. The leakage current I_L decreased with the addition of CeO_2 below 0.3 mole%

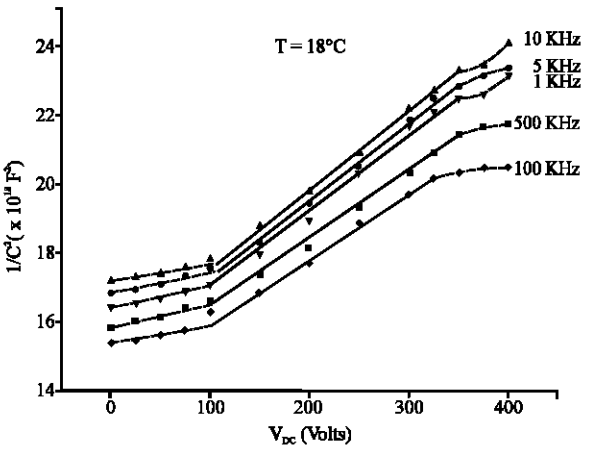

Fig. 4: Mott-Schottky response of the ZnO-Bi_2O_3 based varistor (C1) containing 0.1 mole% CeO_2

and then steadily increased above it. Considering α and I_L concurrently it appears that the C9 sample is somewhat superior among all the samples investigated. This comparative assessment is based on the practical aspect from application considerations as the geometry of the investigated samples is kept the same. The values of E_b, α and I_L for the C9 sample are 425 V mm^{-1}, 35 and 4.8 μA, respectively.

Capacitance-voltage (C-V) behavior: The addition of CeO_2 to a commercial type ZnO-Bi_2O_3 based varistor recipe is systematically studied. The main purpose of presenting the Mott-Schottky plot, i.e., C^{-2} versus V_{DC} plot (Alim *et al*., 1988b; Alim, 1995) in this study is to convey commercial-like features for the recipe investigated. From this response it is clear that this recipe may be used in the commercial purposes.

Figure 4 displays the C-V data at various frequencies of the same sample. An explanation of the observed Mott-Schottky behavior is presented as this device

indicated potential commercial-like features. The frequency-dependence is an indication of the trapping behavior. In general, the C-V study provided no serious indication of the chemically altered grain-to-grain microjunctions but physically CeO_2 aided achieving significant grain size refinement and in turn increment in the electric field. This is an economic approach to achieve high electric field varistors for potential commercialization. The increase in the breakdown electric field which in turn aids to reduce the size of the device for potential application as economics becomes obvious for the CeO_2 added ZnO-Bi_2O_3 based commercial varistor recipe. The improvement may not be too drastic but invariably visible as the increase in the electric field corresponding to the current density in the nonlinear region.

The overall Mott-Schottky response depicts a strong dependence on the applied frequency indicating significant reduction in the terminal capacitance with the increase in measurement frequency. This is identical to the previously investigated commercial and laboratory varistor materials (Alim *et al*., 1988b; Alim, 1995; Morris, 1976; Lei *et al*., 2002, 2004). Each curve exhibits three distinct regions as demonstrated by Alim *et al*. (1988b; Alim, 1995). Usually the low-voltage region (shown as dotted line) corresponds to the ohmic region of the I-V behavior where the net change in the electrical barrier (back-to-back) depletion width (depletion region) across the grain boundaries is nearly unchanged due to the symmetric configuration of the electrical barrier across the grain boundaries. The depletion region gives rise to the geometric capacitance. The linear segment of the Mott-Schottky curve corresponds to the low nonlinear range of the I-V response. The high voltage region (shown as the dotted line) corresponds to the breakdown region of the device. The terminal capacitance loses linearity at these voltage gradients due to the gradual destruction or breakdown of the electrical barriers in the microstructure and thereby enhancing the terminal capacitance. The enhancement is largely contributed by slow departure of the geometric contribution of the depletion regions across the grain boundaries as the narrow increment of the applied voltage is taking place. This demonstrates the firm Schottky barriers within the CeO_2-added ZnO-Bi_2O_3 based varistor materials as reported by Alim *et al*. (1988b), Alim (1995), Li *et al*. (2002) and Morris (1976). This is also confirmed in a recent paper (Lei *et al*., 2004).

The destruction or breakdown of the electrical barriers is a concept for each electrical barrier when attains 3 V to 3.5 V. This voltage range is considered as the breakdown voltage per grain boundary electrical barrier (Bartkowiak *et al*., 1996a, b). It is only a plausible concept that satisfies behavior at low frequencies, as if terminal capacitance is enhanced via gradual elimination of the effect of the junctions with the increment of applied voltage, attributing to the reduced number of junctions for the same operative electrical path between the two opposite electrodes. At high frequencies that effect prevails but reduced magnitude of terminal capacitance is observed presumably due to the systematic elimination of the extraneous contribution (trapping effect) which is predominant at low frequencies. The normalized C-V behavior of the terminal capacitance depicting breakdown responses, both at low and high frequencies, is noted by Lou (1980). Summarizing the observations in the frequency domain two types of distinct response is obtained (Alim *et al*., 1988b; Alim, 1995; Morris, 1976; Li *et al*., 2002):

- The upturn behavior of the Mott-Schottky straight line near to the breakdown voltages usually takes place in the transition range 10 and 100 KHz. For some commercial varistors this range is observed in the vicinity of 50 kHz and attributed to the varistor recipe, processing variables, type of raw materials' suppliers, control of particle size distribution, nature of agglomeration during dispersion, size of the spray dried powder, moisture content of the spray dried powder, etc. The moisture content in the spray dried powder influences the pressing of the varistor blocks which in turn affects the Mott-Schottky plot's upturn (or downturn) including nonlinear response of the I-V behavior at breakdown voltages as a function of frequency.
- The downturn behavior of the Mott-Schottky straight line near to the breakdown voltages is exhibited by the varistors at frequencies lower than 10 kHz. It is quite difficult to get the data often below 500 Hz regardless of the state-of-the-art instrumentation. The difficulty is not associated with the loss tangent (or dissipation factor) handling or capability factor of the instruments. It is difficult to obtain the C-V data at 100 Hz as the Mott-Schottky plot indicates a very short range of the straight line and attributed to the question of stability of the electrical barriers across the grain boundaries. From long time experience in handling ZnO-Bi_2O_3 based varistors, invariably below 100 Hz no meaningful C-V data are obtained. The Mott-Schottky plot's downturn (or upturn) behavior including the nonlinear response of the I-V behavior at breakdown voltages as a function of frequency is attributed to the total aforementioned processing conditions.

No single hypothesis or model satisfies and delineates two foregoing observations for the laboratory and commercial devices. Thus, existing hypotheses or models are not referred. Furthermore, most of these

models are based on simple Debye or singular Debye-like relaxation concept of the conduction processes across the grain boundaries which is indeed never observed in the varistor materials whether prepared in the laboratory or in the manufacturing set-up. Also these varistors do not attribute to the dependence of the recipe specific or processing conditions. As a definite rule, varistor materials always exhibit non-Debye conduction processes up to the applied voltages $V_{1mA.cm^{-2}}$ corresponding to the current density 1 $mAcm^{-2}$. Above $V_{1mA.cm^{-2}}$ the device makes a sharp transition from non-Debye to Debye conduction process and this is demonstrated experimentally by Alim and Seitz (1988). This transition was then attributed to the conduction path channeling that brought the device to a singular Debye-like relaxation. Later the same response was termed as the current localization by Bartkowiak and Mahan (1995). The non-Debye behavior was shown as a partial contribution to the conduction process originally by Levinson and Philipp (1976a) using complex permittivity plane which is often termed as the Cole-Cole plot. This was extended by Alim *et al.* (1988b) identifying contributions of multiple competing trapping phenomena including resonance behavior in a number of commercial varistors.

The varistor materials do not exhibit a single Mott-Schottky straight line regardless of applied frequency (i.e., measurement frequency) like for those observed in the metal-semiconductor (or ideal Schottky barrier diode) devices but show a series of near parallel-like straight lines indicating strong frequency-dependence on the terminal admittance and thus, has no steady C-V response. These Mot-Schottky straight lines appear in such a way that there is a finite variation in the slope (Alim *et al.*, 1988b; Alim, 1995) as a function of measurement frequency.

Due to the complexity of the frequency-dependence of the varistor materials it is not reasonable to attempt extracting a set of device-related parameters from the Mott-Schottky plot using an arbitrary measurement frequency that inherently belongs to the frequency-dependent C-V data. Thus, estimation of the device-related parameters such as built-in-potential (Φ_i), barrer height (Φ_B), grain carrier density (N_d), Femi level position (E_c-E_f), etc. is misleading to the serious investigators. Nevertheless, extracting reasonable-looking device-related parameters using arbitrary single frequency C-V data have no sound physical basis. This is a proven fact for both classical (Muller *et al.*, 2003) and modified (Mukae *et al.*, 1979) forms of the Mott-Schottky equations for arbitrary single frequency C-V data.

Several reasons can account for the limitation in using classical and modified forms of the Mott-Schottky equations for single-frequency C-V data. The measurement frequency is arbitrary even if a sharp transition capacitance, originating from the minimum in dispersion of the terminal admittance (especially terminal parallel capacitance) with ac frequency and the onset of the resonance event, is achieved. This transition capacitance is a potentially erroneous parameter in the C-V analysis. In general, it is greater than the net/total geometric (depletion) capacitance and thus, yields different results for the device-related parameters (Alim *et al.*, 1988b; Alim, 1995). The method of extracting the device-related parameters, using specific single-frequency C-V data and incorporating them into the aforementioned either Mott-Schottky equations, is incorrect at least for the following possible reasons (Alim, 1995):

- Frequency-independent geometric capacitance as a function of dc voltage is not ensured;
- The forward-bias barrier height is not strictly constant;
- The forward-bias barrier does not continuously provide an effect of the electrical field drop (in the forward-bias barrier region) and is thereby unlikely to achieve a flatband situation;
- Trapping states within the depletion layers contribute to the terminal parallel capacitance (at quasi-equilibrium condition) so their contribution is not completely eliminated;
- Continuous/discontinuous trapping and de-trapping under nonequilibrium conditions affecting terminal parallel capacitance;
- Possible leakage of the trapped charges (i.e., destruction of the trap sites) at any instant (i.e., slow or ultra-slow time-dependent processes under AC/DC biasing at a given temperature) which contributes to the conduction processes affecting terminal parallel capacitance;
- The effective cross-sectional area of conduction across the grain-boundary electrical barriers is not precisely known (this area is not necessarily the same as the physical contact area across each grain-boundary);
- Invariant nature of the net/total depletion layer thickness at any instant of a specific experimental situation due to the non-identical grain-boundary junctions (or electrical barriers);
- Nonsymmetric distribution of grain-size and nonsymmetric (or asymmetric) depletion layer thickness involving adjacent grains constituting a back-to-back grain-boundary configuration; and
- Inhomogeneous or random distribution of secondary and other phases at the grain-boundary interfaces resulting into the nonsymmetric/asymmetric trapping contribution in conjunction with the variation in the effective cross-sectional area of conduction affecting terminal parallel capacitance.

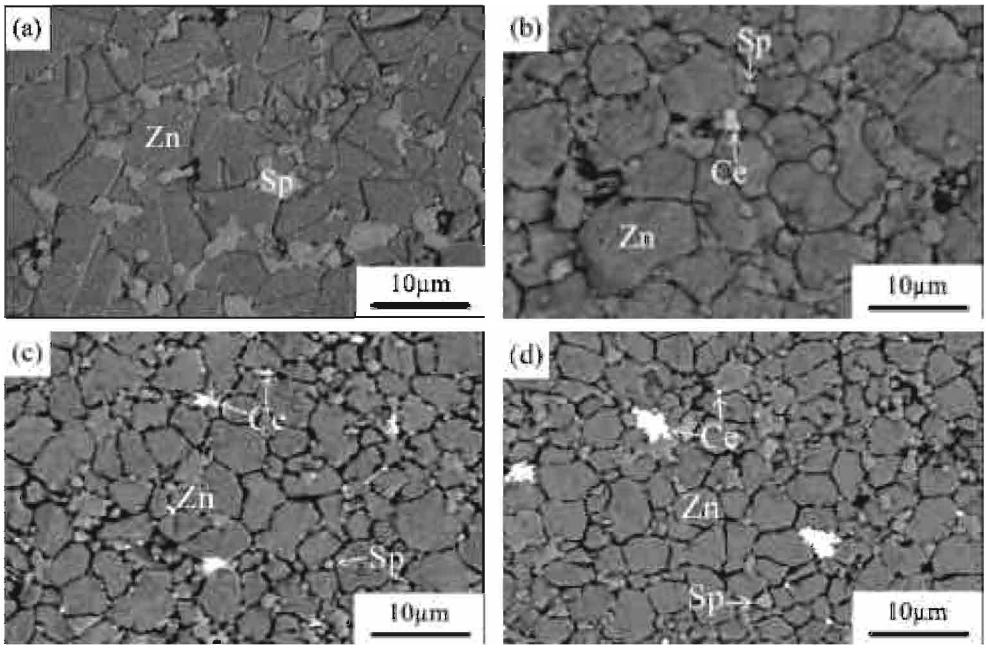

Fig. 5: SEM micrographs of various ZnO-Bi_2O_3 based varistors (a) C0, (b) C1 (c) C3 and (d) C9. (Zn: ZnO phase, Sp: spinel phase, Ce: Ce-rich phase.)

There is no way to delineate or elucidate the frequency-dependent C-V data of the varistor materials without using lumped parameter/complex plane analysis (LP/CPA) technique demonstrated earlier (Alim *et al*., 1988b) to obtain frequency-independent device-related parameters. The LP/CPA technique can only be used if and only if one particular kind of the resonance phenomenon is observed for the device (Alim *et al*., 1988b; Mukae *et al*., 1979). Three distinct types of resonance behavior have been observed in a variety of stable commercial and laboratory devices that are noted and explained by Alim (1993). The resonance behavior demonstrated in this work is identical with that presented by Levinson and Philipp (1976b) and invariably one of the resonance types that Alim (1993) observed.

Microstructural studies: Figure 5 shows the SEM micrographs of four selected samples. In the C0 sample (without CeO_2), two phases designated as the ZnO phase and the spinel phase are observed, whereas in the CeO_2 added samples the existence of an additional phase is evident. Because of the larger atomic number of Ce compared to Zn, the new Ce-rich phase looks brighter and sharper than other areas in Back Scattered Electron (BSE) mode. It distributes mainly at the tri-grain and tetra-grain (or multi-grain) intersections containing ZnO grains and is rarely observed along the grain boundaries bounded by two successive ZnO grains. The physical dimension of this Ce-rich phase is pronounced with increasing CeO_2 content.

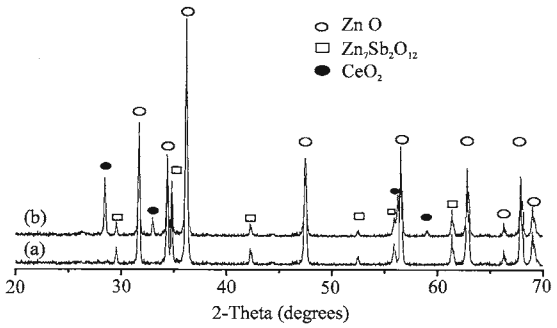

Fig. 6: XRD patterns of ZnO-Bi_2O_3 based samples: (a) without CeO_2 (C0) and (b) with 0.5 mole% CeO_2 (C5)

The powder XRD patterns of selected samples are shown in Fig. 6. The JCPDS cards (ZnO: 5-664; $Zn_7Sb_2O_{12}$: 15-687 and CeO_2: 4-593) were used in the analysis of the phases within the sample. The XRD investigation reveals only two pronounced phases in the C0 (without CeO_2) sample: (1) ZnO phase, (2) $Zn_7Sb_2O_{12}$ spinel phase. However, in the CeO_2 added samples (C5 as a representative since phases observed via XRD in the CeO_2 added samples are identical to the one shown for the

C5 sample), additional peak is evident. Qualitative analysis of XRD attributes the new phase to the addition of CeO_2 in the recipe. No crystallographic Bi_2O_3 peak was observed in any of these samples. This can be explained by a combined effect of a small amount of Bi_2O_3 in the starting stage as well as non-ignorable Bi_2O_3 volatilization during the sintering process. However, during the SEM studies the Bi-rich phase is observed sporadically. Besides, there is no evidence of structural complexities comprising of Bi and Ce.

The exact structure of the Ce-rich particle is not certain at this moment. However, some concepts may be discussed based on the results. It is known that the ionic radius mismatch (Li *et al*., 2002) between Zn^{2+} and Ce^{4+} $[(r_{Zn}^{2+} - r_{Ce}^{4+})/r_{Ce}^{4+}]$ is about -7.22%. The parameter r_{Zn}^{2+} stands for the ionic radius of Zn^{2+} and r_{Ce}^{4+} stands for the ionic radius of Ce^{4+}. Based on the mismatch value ZnO may dissolve into CeO_2 via two mechanisms: (1) vacancy compensation and (2) cation interstitial compensation. Thus a limited solid solution of $Ce_{1-z}Zn_zO_{2-z}$ may have formed by the following solid-state reactions:

$$ZnO \xrightarrow{CeO_2} Zn''_{Ce} + V_O^{\bullet\bullet} + O_O^x, \quad (2)$$

$$2ZnO \xrightarrow{CeO_2} Zn''_{Ce} + Zn_i^{\bullet\bullet} + 2O_O^x, \quad (3)$$

The value of z depends on the solubility of ZnO in CeO_2 and may vary from sample to sample. However, from the morphology of Ce-rich particles in SEM photos, these reactions couldn't have been proceeding in a significant manner. Since the corners and shape of the Ce-rich regions are prominent, it is likely that the solid-state reactions between them and other additives may not have taken place. This is straightforward considering the morphology of the spinel phase which has a flatter interface with the ZnO grains. This indicates intense mutual incorporations between Sb_2O_3 and ZnO, Bi_2O_3 and others must have taken place during sintering. Based on the foregoing discussion it is safe to say that the solid-state reactions between CeO_2 and ZnO, if did occur, were too weak to form a new Ce-Zn-O phase or else. Thus, the Ce-rich regions are essentially CeO_2.

CONCLUSIONS

The CeO_2 addition to the ZnO-Bi_2O_3 based varistor recipe remained chemically nearly affected via I-V and C-V measurements but physically significant pinning at the ZnO grain boundaries caused inhibited grain growth during the sintering process. The average grain size decreased with increasing amount of CeO_2 resulting in a substantial increase in the breakdown field E_b of the samples, while the density of all the well-formed varistor samples was above 95% of the theoretical value. The influence of the CeO_2 addition on the nonlinear coefficient α is very little but the leakage current I_L was improved via enhancing the ohmic resistance and breakdown voltage. Thus, incorporation of CeO_2 is likely to be a way to achieve high electric field ZnO based varistor materials for potential cost effective applications.

REFERENCES

Ai, B., H.T. Nguyên and A. Loubière, 1995. High-field ZnO-based varistors. J. Phys. D: Applied Phys., 28: 774-782.

Alim, M.A. and M.A. Seitz, 1988. Singular nature of preferential conducting paths at high electric fields in ZnO-based varistors. J. Am. Ceramic Soc., 71: C246-C249.

Alim, M.A., M.A. Seitz and R.W. Hirthe, 1988a. Complex plane analysis of trapping phenomena in zinc oxide based varistor grain boundaries. J. Applied Phys., 63: 2337-2345.

Alim, M.A., M.A. Seitz and R.W. Hirthe, 1988b. High-temperature/field alternating-current behavior of ZnO-based varistors. J. Am. Ceramic Soc., 71: C52-C55.

Alim, M.A., 1993. High frequency terminal resonance in ZnO-Bi_2O_3 based varistors. J. Applied Phys., 74: 5850-5853.

Alim, M.A., 1995. An analysis of the mott-schottky behavior in ZnO-Bi_2O_3 based varistors. J. Applied Phys., 78: 4776-4779.

Bartkowiak, M. and G.D. Mahan, 1995. Nonlinear currents in voronoi networks. Phys. Rev., B, 51: 10825-10832.

Bartkowiak, M., G.D. Mahan, F.A. Modine and M.A. Alim, 1996a. Influence of ohmic grain boundaries in ZnO varistors. J. Applied Phys., 79: 273-281.

Bartkowiak, M., G.D. Mahan, F.A. Modine, M.A. Alim, R. Lauf and A. McMillan, 1996b. Voronoi network model of ZnO varistors with different types of grain boundaries. J. Applied Phys., 80: 6516-6522.

Bernik, S., S. Macek and B. Ai, 2001. Microstructural and electrical characteristics of Y_2O_3-doped ZnO-Bi_2O_3-based varistor ceramics. J. Eur. Ceramic Soc., 21: 1875-1878.

Eda, K., 1978. Conduction mechanism of nonohmic zinc oxide ceramics. J. Applied Phys., 49: 2964-2972.

Gupta, T.K., 1990. Application of ZnO oxide varistors. J. Am. Ceramic Soc., 73: 1817-1840.

Lei, M., S. Li, X. Jiao, J. Li and M.A. Alim, 2004. The influence of CeO_2 on the microstructure and electrical behaviour of ZnO-Bi_2O_3 based varistors. J. Phys. D: Applied Phys., 37: 804-812.

Levinson, L.M. and H.R. Philipp, 1976a. High-frequency and high-current studies of metal oxide varistors. J. Applied Phys., 47#7: 3116-3121.

Levinson, L.M. and H.R. Philipp, 1976b. AC properties of metal-oxide varistors. J. Applied Phys., 47#3: 1117-1122.

Levinson, L.M. and H.R. Philipp, 1986. Zinc oxide varistors-A review. Am. Ceramic Soc. Bull., 65: 639-646.

Li, R., S. Yin, S. Yabe, M. Yamashita, S. Momose, S. Yoshida and T. Sato, 2002. Preparation and photochemical properties of nanoparticles of ceria doped with zinc oxide. Bri. Ceramic Trans., 101: 9-13.

Matsuoka, M., 1971. Nonohmic properties of zinc oxide ceramics. Japanese J. Applied Phys., 10: 736-746.

McMillan, A.D., F.A. Modine, R.J. Lauf, M.A. Alim, G.D. Mahan and M. Bartkowiak, 29 December 1998. Rare earth doped zinc oxide varistors. US Patent # 5: 854-586.

Mendelson, M.I., 1969. Average grain size in polycrystalline ceramics. J. Am. Ceramic Soc., 52: 443-446.

Morris, W.G., 1976. Physical properties of the electrical barriers in varistors. J. Vacuum Sci. Technol., 13: 926-931.

Mukae, K., K. Tsuda and I. Nagasawa, 1979. Capacitance-vs-voltage characteristics of ZnO varistors. J. Applied Phys., 50: 4475-4476.

Muller, R.S. and T.I. Kamins and M. Chan, 2003. Device Electronics for Integrated Circuits. 3rd Edn., John Wiley and Sons, Incorporated, NY.

Richmond, W.C., 1980. Electrical characterization of grain boundaries in ZnO-based varistors. Ph.D. Thesis Marquette University, Milwaukee, Wisconsin.

Shichimiya, S., M. Yamaguchi, N. Furuse, M. Kobayashi and S. Ishibe, 1998. Development of Advanced Arresters for GIS with New Zinc-oxide Elements. IEEE Trans. Power Delivery, 13: 465-471.

Viswanath, R.N., S. Ramasamy, R. Ramamoorthy, P. Jayavel and T. Nagarajan, 1995. Preparation and characterization of nanocrystalline ZnO based materials for varistor applications. Nano-Structured Materials, 6: 993-996.

Ya, K.X., H. Yin, T.M. De and T.M. Jing, 1998. Analysis of ZnO varistors prepared from nanosize ZnO precursors. Mat. Res. Bull., 33: 1703-1708.